Research Paper

Polymer Microneedles for Controlled-Release Drug Delivery

Jung-Hwan Park,[1] Mark G. Allen,[2] and Mark R. Prausnitz[1,3,4]

Purpose. As an alternative to hypodermic injection or implantation of controlled-release systems, this study designed and evaluated biodegradable polymer microneedles that encapsulate drug for controlled release in skin and are suitable for self-administration by patients.

Methods. Arrays of microneedles were fabricated out of poly-lactide-*co*-glycolide using a mold-based technique to encapsulate model drugs—calcein and bovine serum albumin (BSA)—either as a single encapsulation within the needle matrix or as a double encapsulation, by first encapsulating the drug within carboxymethylcellulose or poly-L-lactide microparticles and then encapsulating drug-loaded microparticles within needles.

Results. By measuring failure force over a range of conditions, poly-lactide-*co*-glycolide microneedles were shown to exhibit sufficient mechanical strength to insert into human skin. Microneedles were also shown to encapsulate drug at mass fractions up to 10% and to release encapsulated compounds within human cadaver skin. *In vitro* release of calcein and BSA from three different encapsulation formulations was measured over time and was shown to be controlled by the encapsulation method to achieve release kinetics ranging from hours to months. Release was modeled using the Higuchi equation with good agreement ($r^2 \geq 0.90$). After microneedle fabrication at elevated temperature, up to 90% of encapsulated BSA remained in its native state, as determined by measuring effects on primary, secondary, and tertiary protein structure.

Conclusions. Biodegradable polymer microneedles can encapsulate drug to provide controlled-release delivery in skin for hours to months.

KEY WORDS: controlled-release drug delivery; microneedles; protein stability; transdermal drug delivery.

INTRODUCTION

Conventional drug delivery using pills or injection is often not suitable for new protein, DNA, and other therapies (1,2). Devices for controlled release of such compounds have been developed, which enable slow delivery over hours to years. Controlled release is often achieved by encapsulating drugs within biodegradable polymer matrices, from which release is governed by drug diffusion and polymer erosion. Decades of research on this topic have yielded clinical products, such as the Lupron Depot, which delivers leuprolide acetate systemically for months (3), and the Gliadel wafer, which administers carmustine locally to the brain for days to weeks (4).

A limitation, however, of controlled-release systems is that they typically require hypodermic needle injection of polymeric microparticles or possibly surgical implantation of macroscopic devices within the body. These painful and invasive procedures are generally not suitable for self-administration by patients and therefore are limited to use in hospitals or clinics.

The goal of this study was to develop a minimally invasive polymeric controlled-release system suitable for self-administration without the pain or complexity of current controlled-release devices. Rather than using a hypodermic needle to introduce polymeric microparticles into the body, we propose redesigning the microparticles to have the shape of microneedles and thereby give these polymeric particles the functionality of both needles and drug matrices for controlled release (Fig. 1). By integrally forming these microscopic needles onto a patch substrate, arrays of drug-loaded microneedles could be inserted into the skin and worn like a transdermal patch for slow release over time. An alternative approach would involve intentionally separating the patch base from the needles after insertion into the skin, thereby leaving the drug-filled needles invisibly buried in the skin for slow release. Because these microneedles are made of FDA-approved, biodegradable polymer, they should safely disappear after drug delivery is complete. Previous studies have shown that microneedles are painless (5,6).

[1] Wallace H. Coulter Department of Biomedical Engineering at Georgia Tech and Emory University, Georgia Institute of Technology, Atlanta, Georgia 30332, USA.

[2] School of Electrical and Computer Engineering, Georgia Institute of Technology, Atlanta, Georgia 30332, USA.

[3] School of Chemical and Biomolecular Engineering, Georgia Institute of Technology, Atlanta, Georgia 30332, USA.

[4] To whom correspondence should be addressed. (e-mail: prausnitz@gatech.edu)
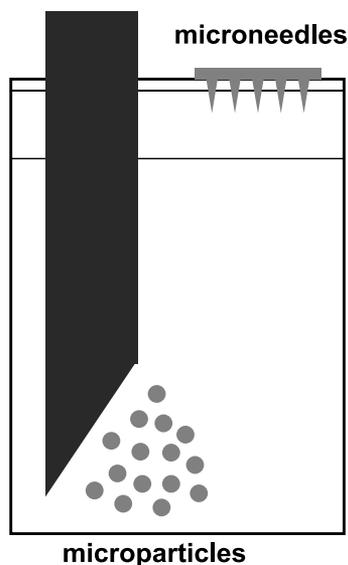
Fig. 1. Controlled-release drug delivery using polymer microneedles. Polymeric controlled release is often achieved by encapsulating drug within microparticles, which are then injected into the body using a hypodermic needle (shown on left). Polymer microneedles can similarly be designed to encapsulate drug for controlled release, but can be directly inserted into the skin without the need for hypodermic injection (shown on right).

Microneedles have previously been proposed and developed for related applications. Solid microneedles have been used to pierce the skin for increased permeability (7) as well as to provide a substrate on which drug can be coated (8) or encapsulated (9) for rapid release. Using this approach, a range of compounds has been delivered to the skin, including proteins, such as insulin and human growth hormone; genetic material, including plasmid DNA and oligonucleotides; and vaccines directed against hepatitis B and anthrax (10,11). Hollow microneedles have also been developed for infusion of drug solutions into the skin (12–14). However, we believe that this is the first study to address the use of microneedles to encapsulate drug for controlled-release delivery (15).

Guided by previous microneedle studies, controlled-release microneedles should measure hundreds of microns in length and have a radius of curvature less than 10 μm at the tip to ensure easy penetration into skin by manual insertion (16). Microneedles of this size can penetrate past the skin's outer barrier of stratum corneum and deliver drug to the epidermis and superficial dermis, where drug can diffuse rapidly for local delivery to skin or systemic distribution via uptake by dermal capillaries. Through the use of biodegradable polymers such as poly-lactide-co-glycolide (PLGA), well-established controlled-release mechanisms can be exploited to control release from microneedles (17,18).

Microneedles of the proposed dimensions can be made by adapting microfabrication technology (19). Although microfabrication often involves lithography and etching of silicon, the field is being expanded to include laser cutting, molding, and other fabrication techniques to produce microdevices made of other materials, including metals and polymers. By leveraging these technologies of the microelectronics industry, methods to make microneedles should provide reproducible mass production at disposable cost.

MATERIALS AND METHODS

Fabrication of Biodegradable Microneedles

Fabrication of Microneedle Master Structures and Molds

Microneedles were fabricated by first making master structures using lithography-based methods, then creating inverse molds of these master structures, and finally preparing replicate microneedles by melting biodegradable polymer formulations into the molds. In this way, one master structure could be used to make multiple molds, which could each be used to make multiple replicates. Microneedles were fabricated using two different geometries: beveled tip and tapered cone. Methods to fabricate these master structures and molds have been described in detail previously (20) and are summarized below.

Beveled-tip microneedle master structures were fabricated out of SU-8 epoxy using standard UV-lithographic techniques (20). SU-8 epoxy (SU-8 100; MicroChem, Newton, MA, USA) was coated onto a silicon wafer and lithographically patterned into cylinders in the shape of the desired needles. The space between the cylinders was filled with a sacrificial polymer (PLGA 85/15, Sigma-Aldrich, St. Louis, MO, USA) and a copper mask was patterned to asymmetrically cover the tops of the epoxy cylinders and some of the sacrificial polymer on one side of each cylinder. Reactive ion etching (RIE; Plasma Therm, St. Petersburg, FL, USA) partially removed the uncovered sacrificial layer and asymmetrically etched the tips of the adjacent epoxy cylinders. All remaining sacrificial polymer was removed by ethyl acetate, leaving an array of epoxy cylinders with asymmetrically beveled tips. This array of needles was coated with poly(dimethylsiloxane) (PDMS; Sylgard 184, Dow Corning, Midland, MI, USA), which was subsequently peeled off to make an inverse mold.

Tapered-cone microneedles were fabricated using a novel microlens technique (Y.-K. Yoon, J.-H. Park, and M. G. Allen. Multidirectional UV lithography for complex 3-D MEMS structures. *J MEMS*, in press). A chromium layer was first deposited and patterned on a glass substrate to form an array of circular dots of exposed glass. Isotropic wet etching of the exposed glass was then performed to create concave wells, which were filled with SU-8 epoxy cast on the surface. The refractive index mismatch between glass and SU-8 epoxy created an array of integrated microlenses. After soft-baking, the SU-8 film was exposed from the bottom (i.e., through the glass) to UV light, which passed through the microlenses to form latent images in the SU-8 epoxy as ray traces from the lenses. After development of the SU-8 epoxy, the resulting tapered-cone microneedle master structure was used to make an inverse PDMS mold.
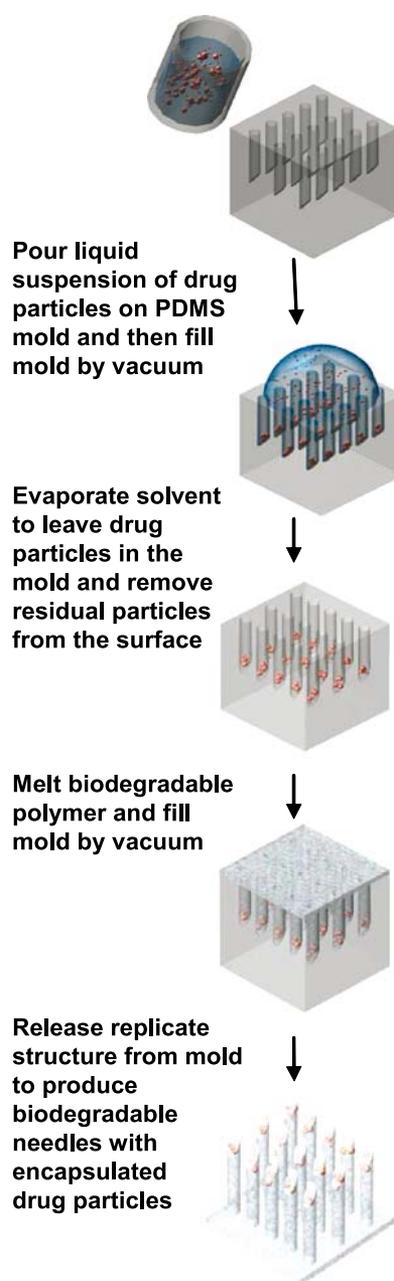
Fabrication of Microneedles Encapsulating Drug

To prepare microneedles encapsulating drug for controlled release, PDMS microneedle molds were first filled with a model drug formulation and then filled with a PLGA melt, which was allowed to cool and solidify. Three formulations were used to achieve different timescales of controlled release. For rapid release, the model drug was

directly encapsulated within the microneedles. For slower release, drug was first encapsulated either within carboxy-methylcellulose (CMC) or poly-L-lactide (PLA), which was then encapsulated within microneedles. The process is summarized in Fig. 2.

For the first formulation, calcein or Texas-Red-labeled bovine serum albumin (BSA) powder (used as received from Sigma-Aldrich or Molecular Probes, Eugene, OR, USA, respectively) was suspended in acetonitrile (Sigma-Aldrich) at a solids content of 10% (w/v) and then homogenized for 5 min at 10,000 rpm (PowerGen 700 homogenizer, Fisher Scientific, Pittsburgh, PA, USA) to make drug microparticles. The homogenized particles, with a broad size distribution over the approximate range of 1–100 μm, were filtered first through a 30-μm filter, and then the filtrate was passed through a 1-μm filter (nylon net filter, Millipore, Billerica, MA, USA). The final solids cake containing particles 1–30 μm in size was redispersed in acetonitrile at a solids content >20% (w/v). The resulting suspension was poured onto a PDMS microneedle mold and placed in a vacuum chamber at −20 kPa for ~5 min. This filled the mold with drug particles by first allowing the vacuum to force the drug suspension into the mold cavities and then evaporate off the organic solvent. Residual particles remaining on the surface of the mold were removed using adhesive tape (Blenderm, 3M, St. Paul, MN, USA). As described previously (20), the mold was then filled with melted PLGA (PLGA 50/50, 1.2 dL/g, Birmingham Polymer, Birmingham, AL, USA) in a vacuum oven at 135°C and −70 kPa for 10–20 min. After cooling, the resulting micro-needles with encapsulated drug were manually removed from the mold.

To retard release from microneedles using a double-encapsulation formulation approach (21), calcein was first encapsulated within CMC microparticles, which were then encapsulated within microneedles. A CMC solution was prepared by dissolving 0.25 g of CMC sodium salt (reference viscosity of 400–800 cP @ 2% aqueous solution; Sigma-Aldrich) in 9.6 mL of deionized (DI) water for 12 h on a 50°C hot plate with stirring at 300 rpm. Then, 25 mg calcein (Sigma-Aldrich) was dissolved in the CMC solution at a calcein: CMC ratio of 1:10 (w/w). The resulting clear solution was poured onto aluminum foil and dried to remove water for 6 h under −50 kPa of vacuum. The resulting film containing calcein dispersed in a solid CMC matrix was pulverized by an agate mortar and pestle to form particles measuring a few hundred microns to a few millimeters in size. These large particles were dispersed in acetonitrile, homogenized, and filtered to yield particles of 1–30 μm in size, as described above. The average diameter of the particles was 9.6 μm, with a standard deviation of 6.2 μm, determined by analyzing scanning electron microscope (SEM) images. The small CMC particles encapsulating calcein were finally loaded into a PDMS mold, which was subsequently filled with PLGA, as described above, to form PLGA microneedles, which encapsulated CMC particles that further encapsulated calcein.

To slow release still more, a similar approach was used, where calcein was first encapsulated within PLA micropar-ticles, which were then encapsulated within microneedles. Using the well-known double-emulsion technique to make PLA microparticles (22), 50 mg of calcein was dissolved in 15 mL DI water and 0.2 g of PLA (L-PLA, 1.0 dL/g; Birming-

Fig. 2. Method to fabricate polymer microneedles that encapsulate drug for controlled release. First, a suspension of drug particles is filled into a microneedle mold. Evaporation of the solvent leaves solid drug particles partially filling the mold. Pellets of biodegradable polymer are then melted into the mold under vacuum. Cooling and solidification of the polymer yields biodegradable polymer micro-needles with encapsulated drug particles.

ham Polymer) was separately dissolved in 2 mL methylene chloride (Sigma-Aldrich). Then, 200 μl of the calcein solution was homogenized in 2 mL of PLA solution for 2 min at 15,000 rpm. The resulting water-in-oil emulsion was homoge-nized in 50 mL of an aqueous solution of 0.1% polyvinyl alcohol (Sigma-Aldrich) for 2 min at 10,000 rpm, which produced a water-in-oil-in-water emulsion. After mixing for 3 h at 300 rpm, the methylene chloride was extracted into the

continuous phase, which solidified the discontinuous phase into PLA microparticles encapsulating calcein. Microparticles of 1–30 μm in size were isolated by filtration, loaded into a PDMS mold, and encapsulated in PLGA microneedles, as described above.

Characterization of Microneedles Containing Drug

In Vitro Release Test in Saline

To measure release rates from microneedles, an array containing 100–200 needles encapsulating one of the formulations of calcein or BSA was attached to the bottom or side of a 30-mL glass vial (All-Pak, Bridgeville, PA, USA) containing 5 or 10 mL of phosphate-buffered saline (PBS, pH 7.4, Sigma-Aldrich) filtered using a 0.2-μm filter (Millipore). Glass vials, PBS, and magnetic stir bars were autoclaved prior to use. The vials were magnetically stirred at 300 rpm and incubated in a 37°C water bath. Periodically, a 100-μl aliquot of PBS was sampled from each vial, replaced with fresh PBS, and analyzed to determine the concentration of calcein or Texas Red-labeled BSA by calibrated spectrofluorometry (QM-1, Photon Technology International, South Brunswick, NJ, USA). Measured concentrations were converted into cumulative drug released (M_t) by accounting for PBS volume. Total drug content (M_0) was determined by placing microneedles in 1 N NaOH overnight at the end of each experiment to fully degrade remaining PLGA and PLA and thereby release all encapsulated drug (23). The resulting solution was returned to pH 7.4 using HCl before analysis. M_0 was typically ∼1 μg for calcein only, BSA only, and calcein in CMC microparticles and ∼0.1 μg for calcein in PLA microparticles.

Drug release from microneedle formulations was modeled using the Higuchi equation (24), which indicates that diffusion-mediated release should be proportional to the square root of time.

$$\frac{M_t}{M_0} = 6\sqrt{\frac{D\tau}{r^2\pi}} \tag{1}$$

In this expression, D is the apparent diffusion coefficient of the drug in the polymer matrix, t is time, and r is the radius of the microneedle (50 μm) (25). This equation was fitted to experimental data to yield D, which is the only unknown (26). The fitting procedure used a least-squares method that minimized the differences between experimental and theoretical values.

In Vitro Release Test in Skin

To study the dissolution and release of drug in skin, microneedles encapsulating calcein were inserted into full-thickness human cadaver skin and placed in a sealed chamber at 4°C. Refrigeration was used to avoid dehydration and degradation of the skin. Recognizing that skin properties and drug delivery kinetics are different at the experimental temperature of 4°C and the body temperature of 37°C, we conducted this experiment to qualitatively verify that our microneedles insert and that encapsulated drug is released in the skin.

After 8 h, the needles were removed and any residual calcein on the skin surface was cleaned off with wet tissue paper. The spatial profile of calcein released in the skin was then imaged by confocal microscopy (LSM 510; Zeiss, Thornwood, NY, USA). Human cadaver skin was obtained from the Emory University Body Donor Program with approval from the Georgia Tech and Emory University Institutional Review Boards.

Microneedle Failure Force Measurement

To determine the effect of calcein encapsulation on microneedle mechanical properties, the microneedle failure force was measured as described previously (16,20). Briefly, stress–strain curves were generated using a displacement-force test station (Model 921A, Tricor Systems, Elgin, IL, USA) while pressing an array of 35 microneedles against a stainless steel surface at a rate of 1.1 mm/s until a preset maximum load (19.6 N) was reached. Microneedles had a base radius of 100 μm, tip radius of 12 μm, and height of 1 mm. Microneedle failure was indicated by a sudden drop in applied force. After each test, microneedles were visually inspected by microscopy to confirm that all microneedles had deformed and failed uniformly. Failure force was determined at calcein contents of 0, 2, and 10% prepared using a single-encapsulation method.

Protein Stability

Because encapsulation of drugs within microneedles involves a brief exposure to a high-temperature polymer melt, the encapsulation process could be damaging to drugs, especially proteins. To assess possible damage, protein stability was tested by measuring protein solubility, dynamic light scattering, and circular dichroism (CD), using BSA as a model protein (27). Because protein content in microneedles is small, larger samples were generated by dispersing 500 mg of homogenized BSA particles in a 27.5 g solution of 10% (w/w) PLGA in acetonitrile and then pouring the suspension onto aluminum foil. A thin polymer film encapsulating BSA particles was formed by evaporating off the acetonitrile for 5 h under −67 kPa vacuum. The film was cut into 3 × 3-cm squares and placed on a 1 cm-thick PDMS film to simulate the molding process. Samples prepared in this way were placed in the oven at 135°C for predetermined times. After cooling, PLGA samples were dissolved again in acetonitrile, and the BSA particles were recovered by filtration, washed with methylene chloride, and dried for 6–8 h under −30 kPa vacuum. Each condition was tested in triplicate.

As a first measure of stability, BSA samples were dissolved in PBS to determine the fraction of BSA remaining soluble after thermal exposure, which includes both native BSA and reversibly denatured BSA. Insoluble aggregates were removed by centrifugation at 23,000 × g for 20 min (28). Protein concentration in the supernatant was determined by the Lowry protein assay (29).

The presence of soluble aggregates of BSA was detected by dynamic light scattering (30). BSA particles were dissolved in PBS at a concentration of 800 μg/mL and filtered to removed insoluble aggregates, and 45 μl of solution was placed in a quartz cuvette (Proterion, now Wyatt Technology, Santa Barbara, CA, USA) at room temperature for

dynamic light scattering measurements (DynaPro-MS/X, Proterion) using CONTIN analysis.

To identify possible changes in the ratio of α-helix/β-sheet components of BSA structure, CD polarimetry measurements were performed using BSA particles dissolved in PBS at a concentration of 70 μg/mL (J700, Jasco, Easton, MD, USA) (31). CD spectra were obtained over a wavelength range of 400–190 nm with a sensitivity of 20 mdeg and a response time of 2 s.

RESULTS

Fabrication of Microneedles for Transdermal Drug Delivery

Fabrication of Microneedle Master Structures

The first step to make polymer microneedles for controlled-release drug delivery involved fabricating master structures using microelectromechanical systems (MEMS) techniques. These master structures were then used to make molds, which were in turn used to make replicate microneedles out of biodegradable polymers. Two different geometries of microneedle master structures were fabricated out of SU-8 epoxy using lithography-based methods. Representative beveled-tip microneedles are shown in Fig. 3A and have a base radius of 50 μm, a tip radius of 5 μm, and a height of 600 μm. The needles are positioned in a 20 × 6 array with a center-to-center spacing between needles of 400 and 1400 μm. The entire array occupies an area of 9 × 9 mm. Geometric parameters of beveled-tip microneedle arrays, such as needle-to-needle spacing, needle base radius, and base shape, were controlled by adjusting the size, shape, and spacing of the lithography mask. The needle height was controlled by the thickness of SU-8 photoresist casting and etching parameters. The tip sharpness was controlled by the etching parameters.
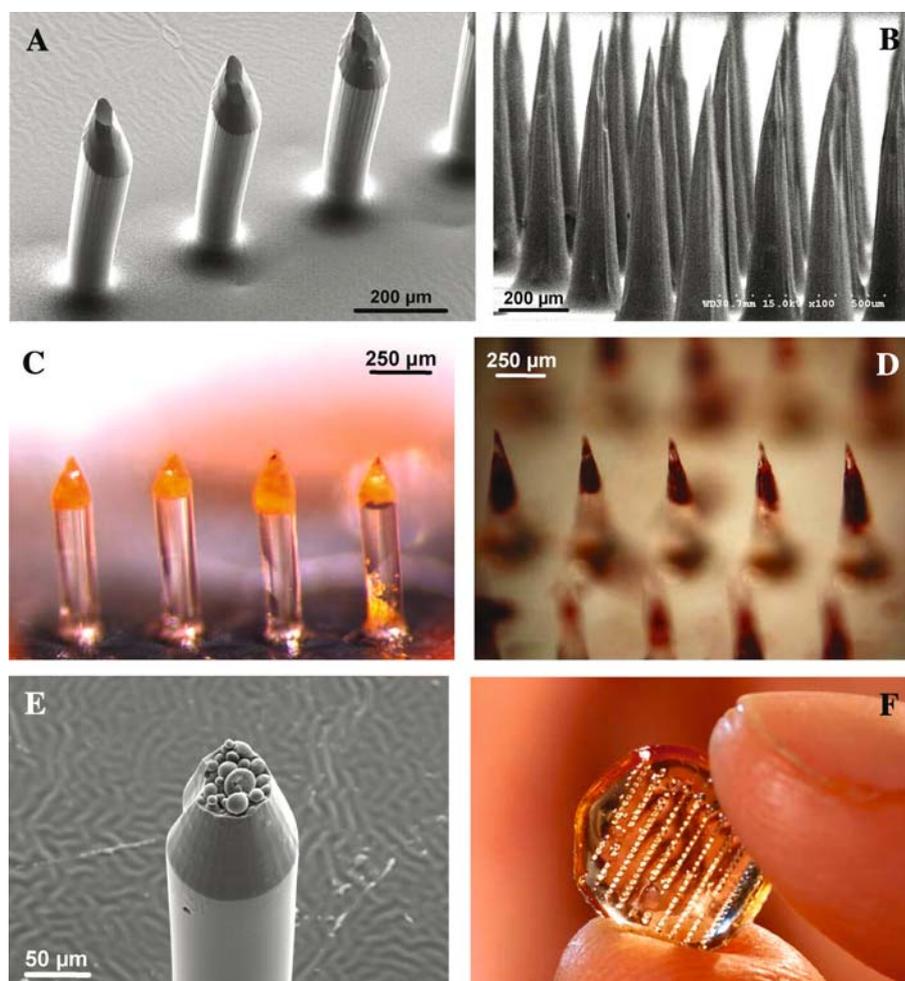
Fig. 3. Microscopy images of microneedles. A section of an array of (A) bevel-tip microneedles and (B) tapered-cone microneedles used as master structures (imaged by SEM). Making a mold and using it to prepare polymer microneedles as described in Fig. 2 yielded (C) bevel-tip and (D) tapered-cone microneedles made of PLGA and encapsulating calcein within their tips (imaged by fluorescence and bright-field microscopy, respectively). Using a double-encapsulation method produced microneedles that encapsulate microparticles that, in turn, encapsulate calcein. (E) Cutting off the tip of a PLGA microneedle reveals the PLA microparticles within (imaged by SEM). (F) A complete 20 × 10 array of PLGA microneedles is shown (imaged by flash photography).

Representative tapered-cone microneedles are shown in Fig. 3B and have a base radius of 100 μm, a tip radius of 2.5 μm, and a height of 750 μm. The needles are positioned in a 10 × 20 array with center-to-center spacing between needles of 400 and 800 μm. The entire array occupies an area of 9 × 9 mm. Needle-to-needle spacing, needle base radius, and base shape were controlled by adjusting the size, shape, and spacing of the lithography mask. Needle height, taper, and tip sharpness were controlled by the optical properties and geometry of the integrated lenses (see "Materials and Methods").

Polymer Microneedles Encapsulating Drug

Using PDMS molds created using the microneedle master structures described above, PLGA microneedles were fabricated with encapsulated calcein or BSA, which served as model drugs. Figure 3C and D shows beveled-tip and tapered-cone microneedles, respectively, with encapsulated calcein. In this case, most calcein was entrapped near the tips of microneedles to be sure that all of the model drug was delivered, even if the microneedles only inserted partially into the skin. Calcein was loaded as solid particles into the microneedles at compositions up to 10% of needle mass. Similar results were seen for encapsulation of BSA in microneedles.

To facilitate slower release, the model drug was first encapsulated either within CMC or PLA microparticles, which were then encapsulated within microneedles. Figure 3E shows a PLGA microneedle with encapsulated PLA microparticles containing 5–10% calcein. The tip of the microneedle has been cut off, thereby exposing the PLA microneedles within. Although these microneedles are made of a solid polymer matrix, a continuous PLGA domain surrounds discrete CMC or PLA microdomains having the size and shape of the microparticles that formed them. To supplement the highly magnified views of microneedles, Fig. 3F shows the size and shape of a complete PLGA microneedle array.

Controlled Release of Drug from Microneedles

Release from Microneedles Using a Single-Encapsulation Formulation

Polymer microneedles encapsulating drugs were developed to serve as a minimally invasive method of controlled-release drug delivery that is similar to injectable microparticulate systems already in clinical use, but does not involve the pain and inconvenience of hypodermic needle injection. To test this idea, controlled release from microneedles loaded with calcein was measured *in vitro*. Using a single-encapsulation formulation (i.e., calcein was directly entrapped within the PLGA matrix of the microneedles), calcein release showed zero-order kinetics over a period of 4 h, after which 93% of encapsulated calcein was released (Fig. 4A). Controlled release of BSA from a similar formulation showed slower kinetics, where 80% of BSA was released after 5 days (Fig. 4A).

These kinetics are consistent with release controlled by drug diffusion through the microneedle polymer matrix, as opposed to release due to polymer degradation and dissolution. First, significant degradation of polymer should not have
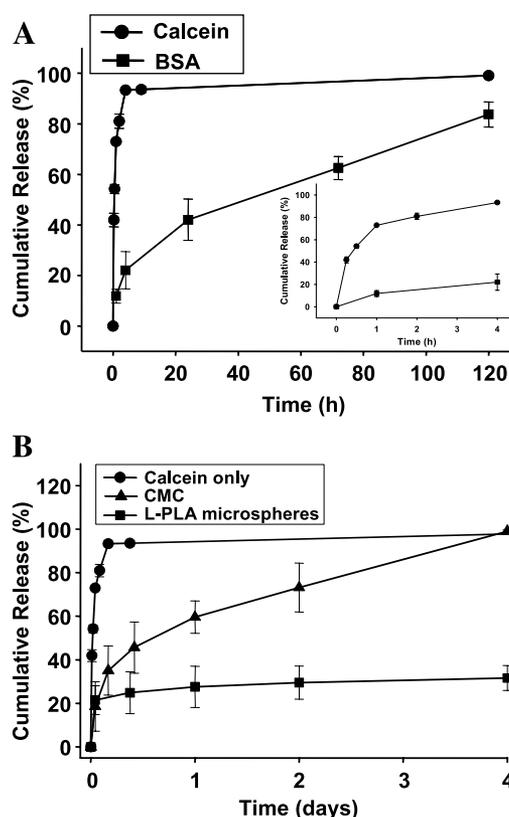
Fig. 4. Cumulative release of model compounds from PLGA microneedles prepared using different formulations to control release kinetics *in vitro*. (A) Release of calcein (●) and BSA (■) encapsulated within microneedles. The inset has an expanded time axis to better show release over the initial 4 h. (B) Release of calcein from microneedles that encapsulated (●) calcein only, (▲) CMC microparticles containing calcein, or (■) PLA microparticles containing calcein. Data are presented as average ± SEM (*n* = 3–5).

occurred over the timescale of hours to days. PLGA degradation is known to occur over a timescale of months (32). This is confirmed by microscopy analysis of microneedles discussed below, which shows that calcein was released before significant needle degradation was observed. Second, degradation-controlled release should be a weak function of drug molecular size (17,18). In contrast, diffusion-controlled release is a strong function of drug molecular size, which is consistent with the order-of-magnitude difference in release rates between calcein and BSA.

As a companion to quantitative release studies, microneedles were imaged by light microscopy during release and degradation. Before release was initiated, calcein was encapsulated within microneedles, especially at the tips, as indicated by the dark regions in the otherwise transparent PLGA microneedles (Fig. 5A). After 9 h of release in PBS, microneedles showed little change in geometry, indicating that significant polymer degradation and dissolution did not yet occur, but were largely devoid of encapsulated calcein, as indicated by the white voids from which calcein was released (Fig. 5B). This image is consistent with release measurements in Fig. 4, which show release kinetics of hours. Subsequent incubation in strong base to rapidly degrade microneedles and fully release any residual entrapped calcein yielded almost fully degraded microneedles (Fig. 5C).
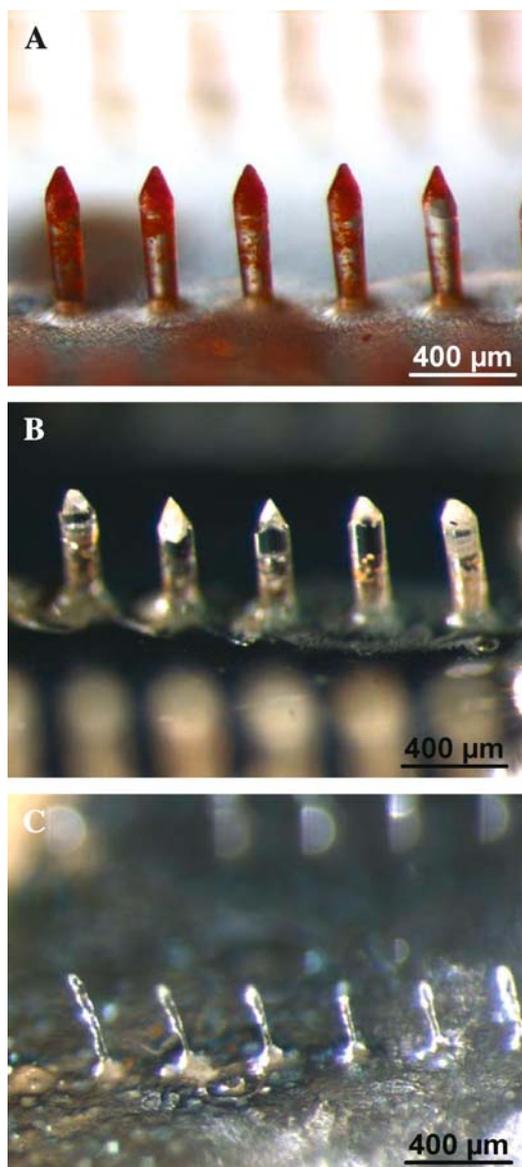
Fig. 5. Microscopic images of microneedles during controlled release and degradation *in vitro* (imaged by bright-field microscopy). (A) Initially, microneedles encapsulated calcein, as indicated by dark regions in the otherwise transparent PLGA microneedles. (B) After incubation in PBS for 9 h, almost all calcein was released from the microneedles, as indicated by the white voids. (C) Incubation in concentrated NaOH rapidly degraded the microneedles and fully released any residual calcein.

Release from Microneedles Using Double-Encapsulation Formulations

To achieve slower release, calcein was first encapsulated within CMC microparticles, which were then encapsulated within PLGA microneedles. Using this approach, calcein release from microneedles showed steady release over 4 days (Fig. 4B). This demonstrates that double encapsulation using CMC can slow release kinetics by more than an order of magnitude. Some calcein may not have been encapsulated within CMC, which could explain the burst effect seen during the first hours of release.

To achieve slow release over a still longer time, calcein was first encapsulated within PLA microparticles, which were then encapsulated within PLGA microneedles. Using this approach, calcein release from microneedles was much slower, exhibiting an initial burst (Fig. 4B), followed by slow release over a 2-month period (discussed below). Although not examined in this study, the double-encapsulation approach lends itself to achieving release over other timescales, which can be controlled by formulation of drugs in microparticles with different polymer compositions using well-known methods (33).

Modeling Controlled Release from Microneedles

Controlled release from polymer matrix systems can be modeled using the Higuchi equation describing Fickian diffusion, which predicts that drug release increases linearly with the square root of time [see Eq. (1)]. This relationship should be valid at times following the initial burst-effect release of nonencapsulated drug and at times before polymer degradation can play a role and the apparent diffusion coefficient is no longer constant. During this release period, the apparent diffusion coefficient of drug inside the microneedles is the only unknown in the Higuchi equation and was determined by nonlinear regression using experimental data for controlled release of calcein and BSA from microneedles with single- and double-encapsulation formulations shown in Fig. 4. Fits of Eq. (1) to these experimental data are shown in Fig. 6. The corresponding correlation coefficients were $r^2 = 0.92$, 0.90, 0.99, and 0.96 for calcein, calcein entrapped in CMC microparticles, calcein entrapped in PLA microparticles, and BSA, respectively.

Based on these fitted equations, the apparent diffusion coefficient of calcein in PLGA microneedles was 1.2×10^{-10} cm²/s (Fig. 6A). The diffusion coefficient of free calcein in water has previously been calculated to be 5.0×10^{-6} cm²/s (13), which is four orders of magnitude greater. Thus, calcein encapsulation within PLGA microneedles significantly slowed calcein diffusion for controlled release. The apparent diffusion coefficient of BSA in PLGA microneedles was 3.0×10^{-12} cm²/s (Fig. 6D), which is five orders of magnitude smaller than free BSA diffusivity in water, 5.9×10^{-7} cm²/s (13). This is again consistent with release controlled by reduced BSA diffusivity in the PLGA matrix.

Encapsulation of calcein in CMC and PLA microparticles reduced the apparent diffusivity still further. CMC encapsulation reduced the diffusivity to 4.7×10^{-12} cm²/s (Fig. 6B), which is more than an order of magnitude lower than without CMC. Encapsulation in PLA microparticles further reduced the diffusion coefficient by another two orders of magnitude to a value of 6.2×10^{-14} cm²/s.

Microneedle Insertion and Controlled Release in Skin

Controlled Release from Microneedles into Skin

Because encapsulated microneedles are envisioned for use in skin, we assessed the ability of microneedles to insert into skin and release drug. In the first experiment, an array of microneedles with encapsulated calcein was inserted into human cadaver skin and then removed after 9 h. Imaging the
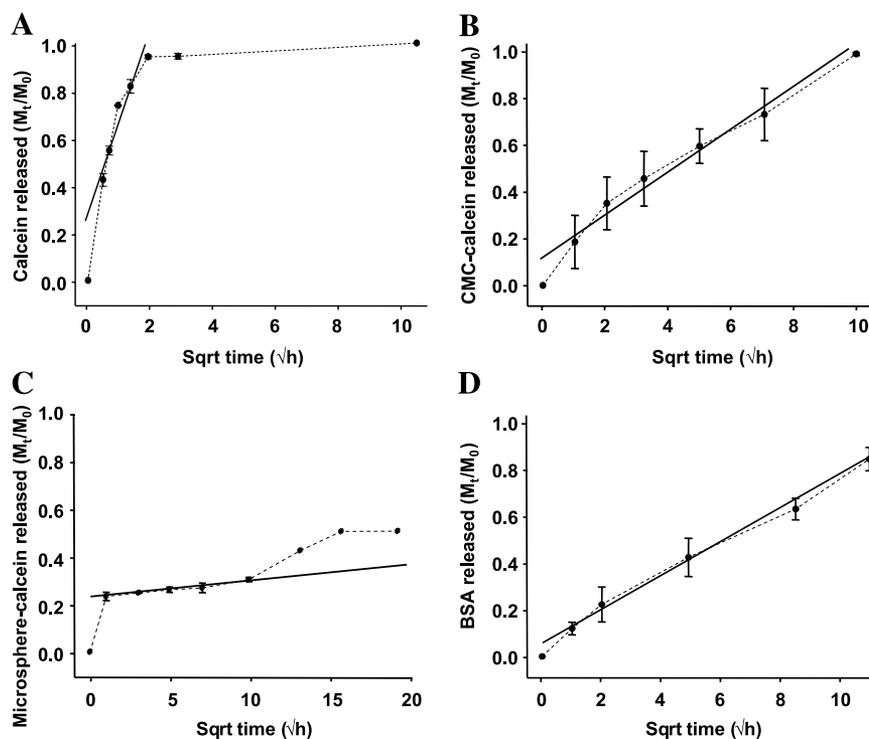
Fig. 6. Modeling of controlled release from PLGA microneedles prepared using different formulations: (A) calcein only, (B) calcein encapsulated in CMC microparticles, (C) calcein encapsulated in PLA microparticles, and (D) BSA only. Data were obtained from Fig. 4. The Higuchi equation (Eq. 1) was fitted to the data, as shown by the solid line. For these fits, the $t = 0$ data points were excluded to eliminate release due to the initial burst effect. In (C), only data up to 100 h were fitted because the effects of polymer degradation became significant at later times. Values of effective diffusivity and correlation coefficients resulting from these fits are presented in the text. The x-axes are presented as the square root of time because the Higuchi equation predicts a linear dependence of release on the square root of time for diffusion-controlled transport.

skin surface by fluorescence microscopy revealed fluorescence at each site of microneedle insertion, indicating that calcein was released into the skin (Fig. 7A). In a companion experiment, skin was treated in the same way and then imaged by confocal microscopy (Fig. 7B). This revealed little fluorescence at the skin surface and intense fluorescence deeper in the skin, with a peak fluorescence at 125–160 μm below the surface, which is just below the dermal–epidermal junction and near the dermal capillary bed (34). This observation further demonstrates that polymer microneedles can release encapsulated compounds within the skin. Because calcein was loaded into the tips of these microneedles, these images also indicate that the microneedles did not insert to their full 750-μm length during this *in vitro* hand insertion. If desired, insertion at higher velocity, with vibration, or with skin under tension (as found on the body *in vivo*) can increase insertion depth by reducing skin deflection during insertion (16,35,36).

Mechanics of Microneedle Insertion into Skin

The ability of microneedles to insert into skin also depends on needle mechanical properties. Although metal microneedles used in other studies are extremely strong, polymer microneedles require special attention to mechanical strength. Our previous study of polymer microneedles (without encapsulated drug) showed that microneedles made of PLGA and other polymers could be designed with sufficient strength for reliable insertion without breaking (20). Because the encapsulation of drug could weaken microneedles, the force required to cause failure of PLGA microneedles was measured at 0, 2, and 10% loading with calcein. As shown in Fig. 8, microneedles without encapsulated drug failed at a force of 163 ± 10 mN per needle. Previous measurements and calculations have shown that needles of the same geometry insert into human skin with a force of 45 mN per needle (16). The safety factor—defined as the ratio of failure force to insertion force—is therefore 3.6, which means that these microneedles insert into the skin with a force much less than the failure force.

Encapsulation of 2% calcein in needles of the same geometry lowered the failure force to 91 ± 30 mN per needle, which indicates that encapsulation weakened the needles, but still maintained a safety factor of 2.0. Encapsulation probably weakened the microneedles because calcein particles are mechanically weaker than PLGA and poor adhesion between calcein particles and the PLGA matrix provided sites for mechanical failure.
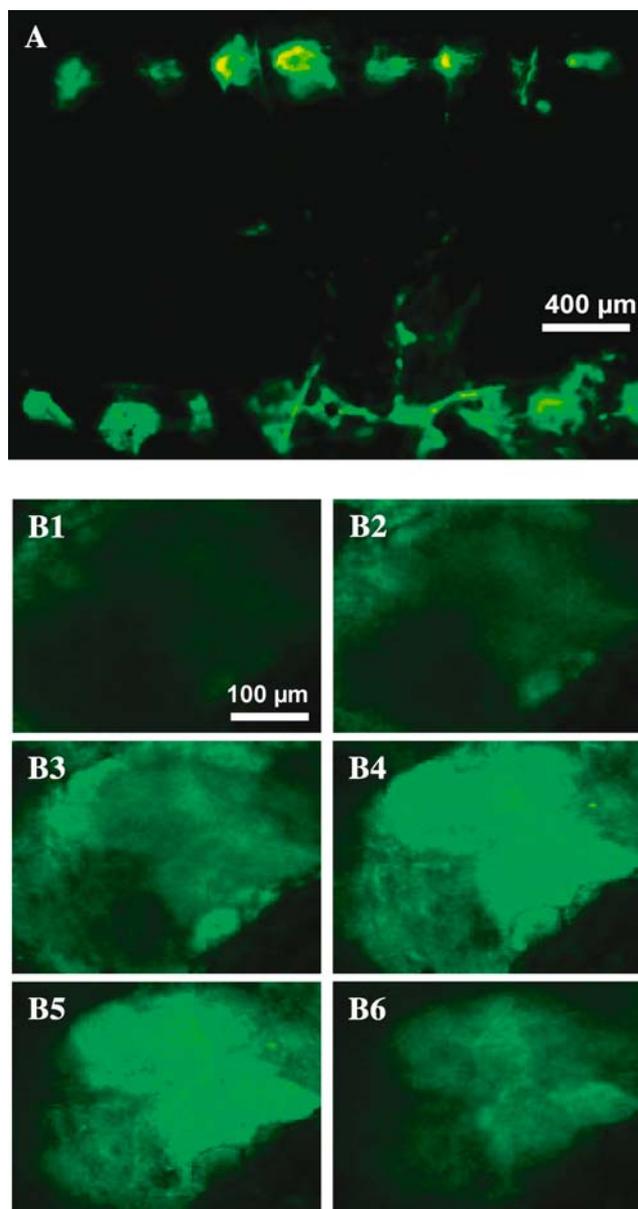
Fig. 7. Fluorescence microscopy images of calcein delivered into human cadaver skin using polymer microneedles. (A) A 100-needle array of PLGA microneedles containing ~1 µg of calcein was inserted into full-thickness cadaver skin for 9 h. After removing the needles, the skin surface was imaged *en face* by fluorescence microscopy, which shows calcein delivery into the skin at the site of each microneedle insertion. (B) Confocal microscopy of the site of one needle insertion shows calcein release within the skin below the skin surface, which is expected for release of calcein encapsulated primarily at the needle tip. Optical section depths are (B1) 20 µm, (B2) 55 µm, (B3) 90 µm, (B4) 125 µm, (B5) 160 µm, (B6) 195 µm below the skin surface.

Encapsulation of 10% calcein lowered the failure force further to 40 ± 2 mN per needle, which reduced the safety factor to 0.89. Because this value is less than 1.0, it means that these microneedles mechanically fail before inserting into skin. However, the microneedles used for this study were relatively blunt (12-µm tip radius) and long (1-mm length). Sharpening tip radius is known to decrease insertion force and shortening needle length is known to increase failure

force (16,20). Thus, it is possible that redesigned PLGA microneedles with 10% drug capsulation might be made strong enough for insertion into skin without failure.

### Protein Stability During Microneedle Fabrication

Encapsulation in microneedles exposed drugs to the high temperature of melted PLGA, which could be damaging, especially to temperature-sensitive proteins. The possibility of damage was reduced by selecting a polymer that can be melted at a relatively low temperature (135°C), minimizing the exposure time to elevated temperature to 10–20 min, and keeping encapsulated drug in the solid state, which reduces conformational mobility and thereby increases protein stability (37). To assess possible protein damage, the effect of exposing BSA to melted PLGA under encapsulation conditions was measured after different exposure times using three different protein stability assays. BSA was chosen as a model protein, although additional studies will be needed to assess stability of other proteins.

First, irreversible denaturation that led to insoluble protein aggregates was assessed by measuring aqueous BSA solubility after various treatments. Exposure to the solvent-based processes used during encapsulation, but without any thermal exposure, did not affect BSA solubility (0 min thermal exposure in Fig. 9A). Exposure to elevated temperature for 10, 20, or 30 min lowered protein solubility by 10, 18, and 32%, respectively, presumably due to irreversible aggregation. After 1 h at elevated temperature, essentially all protein was denatured.

To determine if additional protein aggregates existed among the soluble fraction of BSA, we further tested samples by dynamic light scattering. As shown in Fig. 9B, a 10-min exposure to elevated temperature had no significant effect, whereas 20- and 30-min exposures caused increasing levels of aggregation that formed particles measuring tens of nanometers in size.
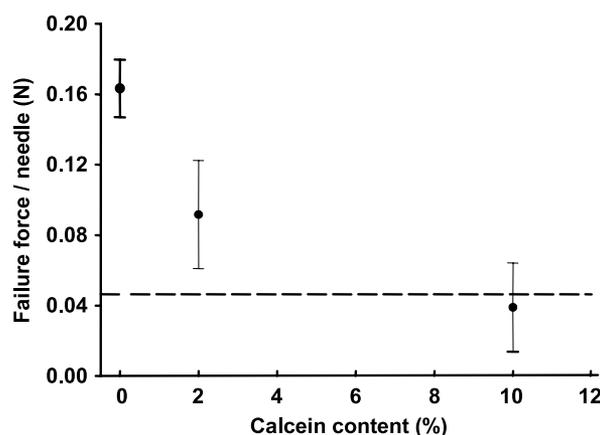
Fig. 8. Mechanical strength of polymer microneedles as a function of calcein encapsulation. The force-per-needle required to fracture an array of 35 microneedles decreased with increasing calcein content. Microneedles had a geometry of 12-µm tip radius, 100-µm base radius, and 1-mm length. The dashed line indicates the expected force required for insertion of a microneedle of these dimensions into skin (16). Data are presented as average ± SEM ($n = 7$).

A

B

C
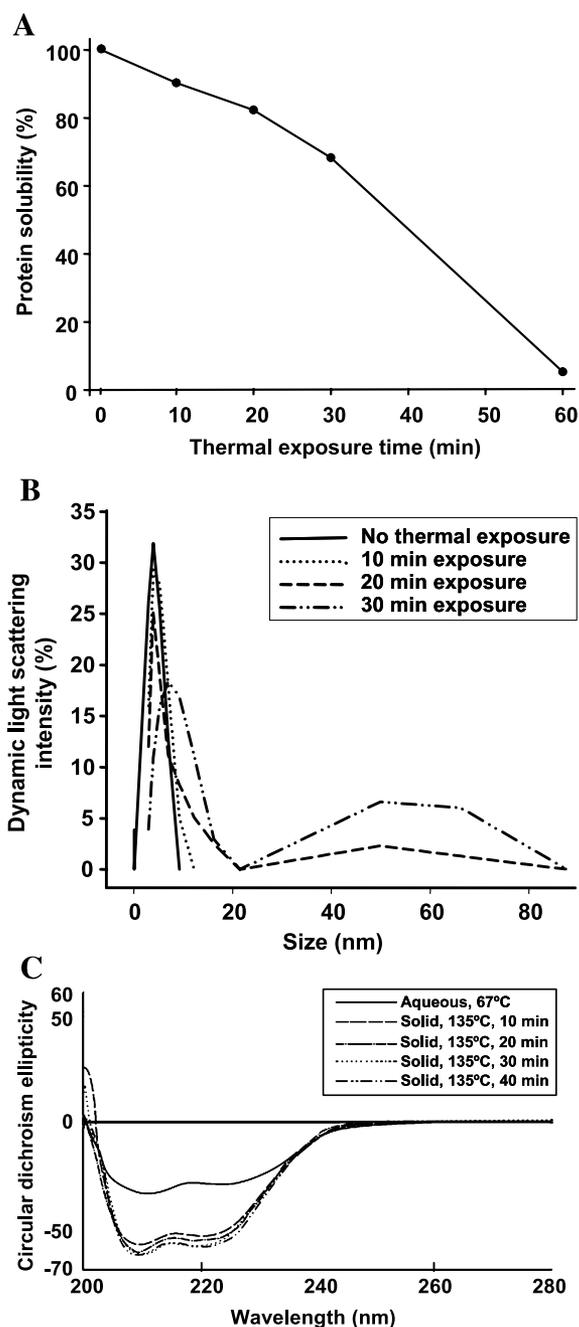
Fig. 9. Stability of BSA after encapsulation within PLGA using thermal exposures similar to those used to fabricate microneedles. (A) BSA solubility in water decreased with increasing length of exposure to the PLGA melt at 135°C. (B) Dynamic light scattering shows that the size distribution of BSA molecules did not change after a 10-min exposure to the PLGA melt, but BSA aggregation was evident after longer exposures. (C) Circular dichroism shows that BSA spectra did not change significantly after exposure of solid-state BSA to the PLGA melt, but BSA in aqueous solution was damaged.

Finally, circular dichroism measurements were made to detect the presence of intermediate species by measuring the ratio of α-helix/β-sheet (27). As shown in Fig. 9C, there was little difference in the spectra of BSA exposed to thermal treatments for up to 30 min, indicating little or no formation of intermediate species. In contrast, a positive control of BSA

incubated in aqueous solution for 25 min at 67°C exhibited a large spectral shift corresponding to significant conformational changes. This observation is consistent with the expectation that keeping protein in the solid state increases stability during thermal processing.

DISCUSSION

Advantages of Controlled Release from Polymer Microneedles

A limitation of conventional controlled-release polymer formulations is that they often require surgical implantation or hypodermic needle injection (1,2). This limits the ability of such systems to be self-administered and generally requires the time and expense of trained clinical personnel. Conventional transdermal patches provide up to 1 week of controlled delivery, but only for the small subset of drugs that can cross skin at useful rates (38). Thus, the possibility of a controlled-release, microneedle-based delivery method could provide a significant advance that captures the ease of use afforded by a patch and the versatile controlled-release properties of biodegradable polymer systems.

Microneedles can be painlessly inserted into the skin in a minimally invasive manner that lends itself to self-administration by patients (5). As designed in this study, the intact microneedle patch could be left in place on the skin for an extended period and later removed. Alternatively, the patch could be designed to intentionally break off the needles, leaving them invisibly embedded in the skin, so that the patch backing could be discarded. In this scenario, microneedles would need to be designed to remain anchored within the skin to prevent unintentional expulsion. By using FDA-approved materials, such as PLGA and CMC, controlled-release microneedles are likely to be safe. By leveraging advanced microelectronics industry fabrication technology, microneedles are likely to be mass-produced at disposable costs (e.g., US$0.10 per patch) (11).

Controlled-release microneedles require no power supply or sophisticated controllers, which also reduces cost and complexity. This contrasts with most other minimally invasive transdermal delivery methods under development (38). Moreover, intersubject variations in skin diffusional barrier properties are less important because delivery is largely controlled by polymer properties of diffusivity and degradation rate. In this study, *in vitro* release kinetics ranging from hours to months were demonstrated using single- and double-encapsulation methods, which should be broadly applicable to many drugs.

Limitations of Controlled Release from Polymer Microneedles

Despite many advantages, controlled-release microneedles have limitations that constrain their possible applications. One disadvantage of the microneedle fabrication method used in this study is that it involves melted polymer that exposes encapsulated drugs to elevated temperature. Although this may not pose difficulties for some small-molecule drugs, this study showed that 10% of encapsulated

BSA was irreversibly aggregated after a 10-min exposure to the polymer melt and that longer exposures led to more extensive denaturation of primary and secondary structure. Thus, applications involving delivery of heat-sensitive drugs are possible, but may lead to partial denaturation. Efforts in our laboratory are underway to develop different methods to fabricate polymer microneedles that do not involve elevated temperatures that damage proteins.

Polymer microneedles for controlled-release delivery are also constrained by needle mechanical properties. Although polymer microneedles can be designed to be strong enough to reliably insert into skin, the addition of encapsulated drug can weaken them. This study found that microneedles with a 2% drug loading retained sufficient mechanical strength, but needles with a 10% loading did not. Although redesign of needle geometry should increase the maximum drug loading that retains needle strength, there is clearly an upper limit, which constrains the maximum possible dose that can be delivered.

Perhaps the greatest shortcoming of controlled-release microneedles is the limited dose that can be administered. Because drug is encapsulated within microneedles and microneedles are, of course, very small, the maximum total dose that can be administered is likely to be less than 1 mg. This estimate is based on the calculation that one microneedle has a mass on the order of 10 μg. Thus, a 100-needle patch with 2% drug loading contains 20 μg of drug. Better needle design may permit a patch with 100–1000 needles loaded with 10% drug, which corresponds to 100–1000 μg. Coating the surface of microneedles could further increase dose.

Although the maximum dose constrains applications, controlled-release delivery of up to 1 mg has a number of candidate drugs on the market, with more likely to be approved in the future. For example, interferon α-2A for hepatitis C, interferon β-1A for multiple sclerosis, and erythropoietin for anemia have doses of 33 μg/week, 132 μg/week and 100 μg/day, respectively (39). Thus, controlled release of 1 mg of drug would last for 30 weeks, 7 weeks, and 10 days, respectively. Vaccine delivery presents another compelling opportunity. For example, hepatitis B vaccine and influenza vaccine require antigen doses of just 10 and 45 μg, respectively. Moreover, the rich dendritic cell population in the skin has been shown to increase immune response to vaccines (40), which provides a further motivation for microneedle-based vaccine delivery to the skin.

CONCLUSION

Polymeric controlled-release drug delivery is a powerful technology with demonstrated clinical utility. To remove the need for administration by clinical personnel, this study developed a microneedle-based controlled-release device designed for self-administration at home. Using this approach, drug can be encapsulated within biodegradable polymer microneedles for controlled release in the skin using fabrication methods designed for inexpensive mass production. Drug-release kinetics ranging from hours to months were controlled by encapsulating drugs directly within the PLGA microneedle matrix or encapsulating drug within CMC or PLA microparticles, which were then encapsulated within the needle. Effective microneedle design required

drug loadings of less than 10% to maintain needle mechanical strength, limited exposure to elevated temperature during needle processing to maintain protein stability, and selection of drugs with total doses less than 1 mg, due to the inherently small size of microneedles. Overall, this study demonstrates the feasibility of using polymer microneedles for controlled-release drug delivery in skin.

REFERENCES

1. R. Langer. Drug delivery and targeting. *Nature* **392**:5–10 (1998).
2. H. Rosen and T. Abribat. The rise and rise of drug delivery. *Nat. Rev. Drug Discov.* **4**:381–385 (2005).
3. P. Periti, T. Mazzei, and E. Mini. Clinical pharmacokinetics of depot leuprorelin. *Clin. Pharmacokinet.* **41**:485–504 (2002).
4. H. Brem, S. Piantadosi, P. C. Burger, M. Walker, R. Selker, N. A. Vick, K. Black, M. Sisti, S. Brem, and G. Mohr, *et al.* Placebo- controlled trial of safety and efficacy of intraoperative controlled delivery by biodegradable polymers of chemotherapy for recurrent gliomas. The Polymer-Brain Tumor Treatment Group. *Lancet* **345**:1008–1012 (1995).
5. S. Kaushik, A. H. Hord, D. D. Denson, D. V. McAllister, S. Smitra, M. G. Allen, and M. R. Prausnitz. Lack of pain associated with microfabricated microneedles. *Anesth. Analg.* **92**:502–504 (2001).
6. J. A. Mikszta, J. B. Alarcon, J. M. Brittingham, D. E. Sutter, R. J. Pettis, and N. G. Harvey. Improved genetic immunization via micromechanical disruption of skin-barrier function and targeted epidermal delivery. *Nat. Med.* **8**:415–419 (2002).
7. S. Henry, D. McAllister, M. G. Allen, and M. R. Prausnitz. Microfabricated microneedles: a novel method to increase transdermal drug delivery. *J. Pharm. Sci.* **87**:922–925 (1998).
8. M. Cormier, B. Johnson, M. Ameri, K. Nyam, L. Libiran, D. D. Zhang, and P. Daddona. Transdermal delivery of desmopressin using a coated microneedle array patch system. *J. Control. Release* **97**:503–511 (2004).
9. T. Miyano, Y. Tobinaga, T. Kanno, Y. Matsuzaki, H. Takeda, M. Wakui, and K. Hanada. Sugar micro needles as transdermic drug delivery system. *Biomed. Microdevices* **7**:185–188 (2005).
10. M. R. Prausnitz. Microneedles for transdermal drug delivery. *Adv. Drug Deliv. Rev.* **56**:581–587 (2004).
11. M. Prausnitz, J. Mikszta, and J. Raeder-Devens. Microneedles. In E. Smith and H. Maibach (ed.), *Percutaneous Penetration Enhancers*, CRC Press, Boca Raton, FL, 2005, pp. 239–255.
12. J. G. E. Gardeniers, R. Luttge, J. W. Berenschot, M. J. de Boer, Y. Yeshurun, M. Hefetz, R. van't Oever, and A. van den Berg. Silicon micromachined hollow microneedles for transdermal liquid transport. *J. MEMS* **6**:855–862 (2003).
13. D. V. McAllister, P. M. Wang, S. P. Davis, J.-H. Park, P. J. Canatella, M. G. Allen, and M. R. Prausnitz. Microfabricated needles for transdermal delivery of macromolecules and nanoparticles: fabrication methods and transport studies. *Proc. Natl. Acad. Sci. USA* **100**:13755–13760 (2003).
14. R. K. Sivamani, B. Stoeber, G. C. Wu, H. Zhai, D. Liepmann, and H. Maibach. Clinical microneedle injection of methyl nicotinate: stratum corneum penetration. *Skin Res. Technol.* **11**:152–156 (2005).

15. J. H. Park, S. P. Davis, Y. K. Yoon, M. R. Prausnitz, and M. G. Allen. Micromachined biodegradable microstructures. In *The 16th Annual International Conference on Micro Electro Mechanical Systems*, IEEE, Piscataway, NJ, 2003, pp. 371–374.

16. S. P. Davis, B. J. Landis, Z. H. Adams, M. G. Allen, and M. R. Prausnitz. Insertion of microneedles into skin: measurement and prediction of insertion force and needle fracture force. *J. Biomech.* **37**:1155–1163 (2004).

17. W. M. Saltzman. *Drug Delivery: Engineering Principles for Drug Therapy*, Oxford University Press, New York, 2001.

18. D. G. Kanjickal and S. T. Lopina. Modeling of drug release from polymeric delivery systems—a review. *Crit. Rev. Ther. Drug Carr. Syst.* **21**:345–386 (2004).

19. M. J. Madou. *Fundamentals of Microfabrication: The Science of Miniaturization*, CRC Press, Boca Raton, FL, 2002.

20. J.-H. Park, M. G. Allen, and M. R. Prausnitz. Biodegradable polymer microneedles: fabrication, mechanics and transdermal drug delivery. *J. Control. Release* **104**:51–66 (2005).

21. H. K. Lee, J. H. Park, and K. C. Kwon. Double-walled microparticles for single shot vaccine. *J. Control. Release* **44**:283–293 (1997).

22. J.-P. Benoit, H. Marchais, H. Rolland, and V. V. Velde. Biodegradable microspheres: advances in production technology. In S. Benita (ed.), *Microencapsulation*, Marcel Dekker, New York, 1996, pp. 35–72.

23. R. K. Gupta, A. C. Chang, P. Griffin, R. Rivera, Y. Y. Guo, and G. R. Siber. Determination of protein loading in biodegradable polymer microspheres containing tetanus toxoid. *Vaccine* **15**:672–678 (1997).

24. Y. W. Chien (ed.), *Novel Drug Delivery Systems: Fundamentals, Developmental Concepts, Biomedical Assessments*, Marcel Dekker, New York, 1991.

25. R. W. Baker and H. K. Lonsdale. Controlled release: mechanisms and rates. In A. C. Tanquary and R. E. Lacey (ed.), *Controlled Release of Biologically Active Agents. Advances in Experimental Medicine and Biology,* Vol. 47, Plenum Press, New York, 1974, pp. 15–72.

26. N. Faisant, J. Siepmann, and J. P. Benoit. PLGA-based microparticles: elucidation of mechanisms and a new, simple mathematical model quantifying drug release. *Eur. J. Pharm. Sci.* **15**:355–366 (2002).

27. D. Bulone, V. Martorana, and P. L. San Biagio. Effects of intermediates on aggregation of native bovine serum albumin. *Biophys. Chem.* **91**:61–69 (2001).

28. W. R. Liu, R. Langer, and A. M. Klibanov. Moisture-induced aggregation of lyophilized proteins in the solid state. *Biotechnol. Bioeng.* **37**:177–184 (1991).

29. O. H. Lowry, N. J. Rosebrough, A. L. Farr, and R. J. Randall. Protein measurement with the Folin phenol reagent. *J. Biol. Chem.* **193**:265–275 (1951).

30. B. J. Berne and R. Pecora. *Dynamic Light Scattering: With Applications to Chemistry, Biology, and Physics*, Dover Publications, Mineola, NY, 2000.

31. G. D. Fasman (ed.). *Circular Dichroism and the Conformational Analysis of Biomolecules*. Plenum, New York, 1996.

32. L. Lu, C. A. Garcia, and A. G. Mikos. *In vitro* degradation of thin poly(DL-lactic-co-glycolic acid) films. *J. Biomed. Mater. Res.* **46**:236–244 (1999).

33. K. Park (ed.), *Controlled Drug Delivery: Challenges and Strategies*. American Chemical Society, Washington, DC, 1997.

34. N. A. Monteiro-Riviere. Comparative anatomy, physiology, and biochemistry of mammalian skin. In D. W. Hobson (ed.), *Dermal and Ocular Toxicology*, CRC Press, Boca Raton, FL, 1991, pp. 3–71.

35. P. J. Rousche and R. A. Normann. A method for pneumatically inserting an array of penetrating electrodes into cortical tissue. *Ann. Biomed. Eng.* **20**:413–422 (1992).

36. M. Yang and J. D. Zahn. Microneedle insertion force reduction using vibratory actuation. *Biomed. Microdevices* **6**:177–182 (2004).

37. T. Arakawa, S. J. Prestrelski, W. C. Kenney, and J. F. Carpenter. Factors affecting short-term and long-term stabilities of proteins. *Adv. Drug Deliv. Rev.* **46**:307–326 (2001).

38. M. R. Prausnitz, S. Mitragotri, and R. Langer. Current status and future potential of transdermal drug delivery. *Nat. Rev. Drug Discov.* **3**:115–124 (2004).

39. *Physicians' Desk Reference*. Thomson PDR, Montvale, NJ, 2005.

40. S. Mitragotri. Immunization without needles. *Nat. Rev. Immunol.* **5**:905–916 (2005).